Solid State Communications 150 (2010) 2134–2137

Contents lists available at ScienceDirect

Solid State Communications

journal homepage: www.elsevier.com/locate/ssc

Charge density waves in $NbSe_3$: The models and the experimental evidence

A. Prodan [a,*], H.J.P. van Midden [a], R. Žitko [a], E. Zupanič [a], J.C. Bennett [b], H. Böhm [c]

[a] Jožef Stefan Institute, Ljubljana, Slovenia
[b] Department of Physics, Acadia University, Wolfville, Nova Scotia, Canada B0P 1X0
[c] Geosciences, University of Mainz, D-55099 Mainz, Germany

ARTICLE INFO

Article history:
Received 2 July 2010
Received in revised form
6 September 2010
Accepted 8 September 2010
by P. Sheng
Available online 17 September 2010

Keywords:
A. $NbSe_3$
B. Low-dimensional structures
C. Charge density waves

ABSTRACT

Charge density wave (CDW) ordering in the prototypical low-dimensional compound $NbSe_3$ is reconsidered. It is shown that the model with two incommensurate modulations, $\boldsymbol{q}_1 = (0, 0.241, 0)$ and $\boldsymbol{q}_2 = (0.5, 0.260, 0.5)$, localized on type-III and type-I bi-capped trigonal prismatic columns, does not explain details, revealed by various microscopic methods. An alternative explanation, based on the existence of modulated layered nano-domains below both CDW onset temperatures, is suggested. It accounts for the presence of the $\boldsymbol{q}_2$ modulation in the STM images recorded above the T_2 CDW transition and for the absence of $\boldsymbol{q}_2$ satellites in the corresponding diffraction patterns. The long periodic modulation, detected by LT STM, is attributed to a beating between the two CDWs, centered on adjacent columns of the same type. Such pairs of alternatively modulated columns represent the basic modulation units, ordered into nano-domains.

1. Introduction

Only a relatively small group of one-dimensional (1-D) compounds exhibits charge density wave (CDW) sliding under the application of an external electric field. This group includes in addition to the most thoroughly studied $NbSe_3$ also its isostructural monoclinic polymorph *m*-TaS_3 [1], NbS_3 [2], $(TaSe_4)I$ [3], $(NbSe_4)_{10}I_3$ [4], the "blue bronzes" $A_{0.3}MoO_3$ with A = K, Rb, Tl [5–8] and the organic conductor TTF-TCNQ [9]. It was shown recently [10] that X-ray crystallography breaks down for structures in which order extends over nanometers only. $NbSe_3$ is a typical example where the extent of order in its modulated structure may be of crucial importance for its physical properties. We thus reconsider in the present work the available experimental evidence, particularly the low-temperature (*LT*) scanning tunneling microscopic (STM) results and give a concurrent explanation for the CDW ordering in this compound.

2. The basic structure

The $NbSe_3$ room-temperature (*RT*) basic structure [11] is reproduced in Fig. 1. The unit cell contains three types of symmetry-related pairs of bi-capped trigonal prismatic (BCTP) columns. These are formed of Nb chains in Se cages, aligned parallel to the monoclinic $\boldsymbol{b_0}$-direction. The inter-column covalent bonding forms corrugated layers parallel to the $\boldsymbol{b_0}$–$\boldsymbol{c_0}$ monoclinic plane, separated by van der Waals (vdW) gaps. Thus, the structure is strongly anisotropic: in addition to the 1-D nature characterized by the BCTP columns, it also shows a pronounced two-dimensional character. Among the three different types of BCTP columns the type-I and type-III ones are similar, with equilateral bases, while the bridging type-II columns appear more regular, with almost isosceles-like bases.

3. The CDW models

It was argued [12] that two incommensurate (IC) CDWs appear independently at different onset temperatures along two of the three available BCTP columns: $\boldsymbol{q_1} = (0, 0.241, 0)$ below $T_1 = 144$ K along type-III and $\boldsymbol{q}_2 = (0.5, 0.260, 0.5)$ below $T_2 = 59$ K along type-I columns. Such CDW formation and ordering appeared to be in good accord with a variety of experiments performed on $NbSe_3$, including nonlinear transport properties [13–27], electron [28] and X-ray diffraction studies [29–32], nuclear magnetic resonance (NMR) [33–35] and angular resolved photoemission spectroscopy [36,37]. However, the model seems to be in disaccord with some transmission electron microscopy (TEM) [38] and particularly LT STM observations [39–42].

It was alternatively suggested [43] that both IC CDWs are formed simultaneously and statistically along type-I columns below T_1 and in addition along type-III columns below T_2. Highly anisotropic and unstable layered nano-domains, oriented parallel to the vdW gaps, are supposed to be formed as a result of the CDW

* Corresponding address: Condensed Matter Physics, Jožef Stefan Institute, Jamova 39, 1000 Ljubljana, Slovenia. Tel.: +386 1 4773 552; fax: +386 1 2519 385.
E-mail address: albert.prodan@ijs.si (A. Prodan).

0038-1098/$ – see front matter © 2010 Elsevier Ltd. All rights reserved.
doi:10.1016/j.ssc.2010.09.010

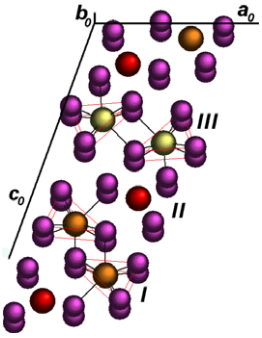

Fig. 1. The structure of $NbSe_3$ [11]. Red (dark), orange (gray) and yellow (light) balls represent Nb atoms along type-II, type-I and type-III columns and the small violet (dark) balls show Se atoms. Nb coordination in the type-I and type-III columns is indicated. (For interpretation of the references to colour in this figure legend, the reader is referred to the web version of this article.)

ordering. This model is based on two conditions: first, the domains must be sufficiently small to extinguish the $\boldsymbol{q_2}$ contribution to the diffraction pattern between T_1 and T_2 and second, they must be in proper phase relationships.

4. The experimental evidence

X-ray and electron diffraction: Diffuse precursor scattering was first reported in electron diffraction patterns of $NbSe_3$ at temperatures above the $\boldsymbol{q_1}$ CDW transition [28]. Next, several X-ray analyses were performed on both, the $\boldsymbol{q_1}$ and $\boldsymbol{q_2}$ satellites. From the line widths of both types of satellites an anisotropy between the correlation lengths ξ_{b^*} and ξ_{a^*} (i.e. parallel to the chains and perpendicular to the cleavage planes) was found [29]. A few degrees above T_1 and T_2 the parallel values were estimated as $\xi_{b^*} > 5$ nm (measured on a $\boldsymbol{q_1}$ satellite at 160 K) and $\xi_{b^*} > 10$ nm (measured on a $\boldsymbol{q_2}$ satellite at 62 K) and the corresponding perpendicular values as $\xi_{a^*} \approx 1.2$ nm and $\xi_{a^*} \approx 3$ nm. Resolution limited correlation lengths of $\xi_{b^*} > 280$ nm at 80 K (i.e. below T_1) and $\xi_{b^*} \approx 70$ nm at 155 K for scans along $\boldsymbol{b_0^*}$ and $\xi_{a^*} \approx 4.2$ nm, $\xi_{b^*} \approx 14$ nm and $\xi_{c^*} \approx 0.5$ nm for the transverse scans along $\boldsymbol{a_0^*}$ (at about 6 K above T_1), were determined for the $\boldsymbol{q_1}$ satellites, with a slight variation of $\boldsymbol{q_1}$ between T_1 and 80 K [30]. Pretransitional structural fluctuations were detected for both, $\boldsymbol{q_1}$ and $\boldsymbol{q_2}$ satellites [31], with a smaller anisotropy for the $\boldsymbol{q_2}$ satellites (1:3.5:6) as compared to the one of the $\boldsymbol{q_1}$ satellites (1:4:20) (both ratios given along the perpendicular $\boldsymbol{b_0}$, $\boldsymbol{a_0}$, and $\boldsymbol{c_0^*}$ directions). Similar intrachain ξ_b and interchain ξ_a correlation lengths were found for both CDWs a few degrees above the transition temperatures, while the corresponding ξ_{c^*} values were at larger variance. Approximate values for the $\boldsymbol{q_2}$ satellites at 65 K, deduced from [31], are $\xi_b \approx 6.5$ nm, $\xi_a \approx 2$ nm and $\xi_{c^*} \approx 1.5$ nm. These correlation lengths, particularly those measured perpendicular to the chains, indeed appear short in comparison with the coherence regions, whose estimated sizes extend for synchrotron X-rays radiation to 125 nm [44] and for high-energy electrons in TEM experiments to 380 nm [45].

In a synchrotron radiation analysis [32] the atomic displacements along the three BCTP columns were found to be in accord with the original Wilson's model. However, if segments of variable lengths along the type-III (below T_1) and in addition along the type-I columns (below T_2) are allowed to be alternatively modulated by the $\boldsymbol{q_1}$ and $\boldsymbol{q_2}$ modes, as suggested in the domain model, the overall contribution to the reciprocal space would appear identical for both models. The same arguments apply also for any high energy electron diffraction experiments. Consequently, both models will not be distinguished on the basis of the diffraction experiments.

NMR: NMR measurements were performed at room temperature (*RT*), 77 K (LNT) and 4.2 K (LHeT) on powdered samples and on samples composed of a large number of aligned crystals [33–35]. The ^{93}Nb (I = 9/2) spectra recorded at RT with the magnetic field parallel to the crystallographic $\boldsymbol{b_0}$ direction resolved 27 lines, which clearly corresponded to the three different Nb sites. While one set of lines remained unchanged on cooling, the second became smeared at LNT and the third in addition at LHeT. This is in accord with the original model [12], where the Nb sites of the type-II columns are not modulated, while the $\boldsymbol{q_1}$ CDW appears on cooling below T_1 along the type-III and in addition the $\boldsymbol{q_2}$ CDW below T_2 along the remaining type-I columns. However, NMR does not distinguish the Nb sites with regard to $\boldsymbol{q_1}$ and $\boldsymbol{q_2}$. Thus, the behavior is also in accord with the domain model [43].

TEM: In addition to high-energy electron diffraction studies [28], satellite dark field TEM [38] was also performed on $NbSe_3$. Elongated strands, in average 20 nm wide and 2000 nm long, crossed by unstable Moiré-like fringes between 8 nm and a few 100 nm wide, were observed in samples cooled to temperatures both above and below T_2. The strands and fringes exhibited a characteristic "twinkling", whose appearance above T_2 could not be explained on basis of the original Wilson's model.

LT STM: The main problem with LT STM images [40–42] remains their dependence on the tunneling parameters, which influence the detected CDWs. In addition, subsurface effects are often superimposed onto the surface contribution, which complicates the interpretation. Nevertheless, a few important details should be pointed out:

1. Dependent on temperature, all images reveal one (type-III) or two (type-III and type-I) strongly modulated BCTP columns per $\boldsymbol{c_0}$ periodicity.
2. The intensity of the CDWs depends on the polarity of the applied gap voltage.
3. Adjacent strongly modulated columns are either ordered in-phase (in case a single column appears per $\boldsymbol{c_0}$) or out-of-phase (if these appear in pairs).
4. All modulated surface columns show within the well ordered regions the same CDW periodicity.
5. There is always one mode present (either as a strong surface modulation or as a weak subsurface contribution), whose ordering enlarges the lateral periodicity into $2\boldsymbol{c_0}$.

Points 1–3 are in agreement with either of the two models, while 4 and 5 support the domain model, possibly with some modifications. The first LT STM image shown [39] reveals pairs of strongly modulated out-of-phase chains with a $2\boldsymbol{c_0}$ lateral periodicity. These pairs can only represent type-III and type-I columns, modulated by the same $\boldsymbol{q_2}$ CDW. What may appear at variance with the suggested domain model [43] are the remaining single weakly modulated columns. According to their position and intensity they represent subsurface columns, which form pairs with the same type of the adjacent surface columns. Their modulation periodicity appears slightly larger in comparison with the surface columns and can only show in-phase ordered $\boldsymbol{q_1}$ CDWs. According to their position the adjacent surface–subsurface pairs represent the type-I columns. If so, the remaining nonmodulated chains represent surface type-II columns. Although these details are in accord with the basic supposition of the domain model, i.e. the existence of layered domains with both type-III and type-I columns modulated by either of the two CDWs, they appear in disaccord with the prediction that the same CDWs occupy strongly bonded pairs of columns. Instead, these details rather indicate that the double layers are composed of $\boldsymbol{q_1}$ and $\boldsymbol{q_2}$ sublayers.

5. Discussion

LT STM is of particular importance, because it is basically different from the alternative methods, including high-resolution

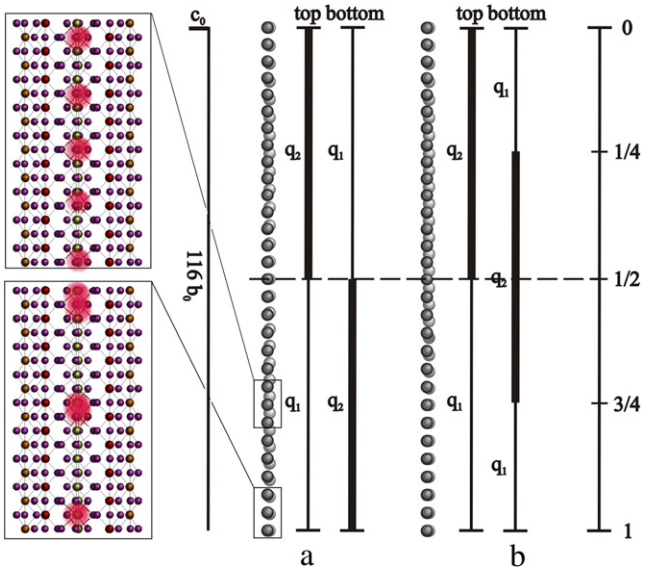

Fig. 2. A model of possible combined $\boldsymbol{q_1}$ and $\boldsymbol{q_2}$ modulations along two adjacent $NbSe_3$ type-III columns (a) and after the $\boldsymbol{q_2}$ part was displaced along the lower column by π (b).

TEM. Although many approaches are beyond any doubt capable of achieving atomic resolution, STM and other scanning probe microscopies are the only methods where information is not collected statistically over a relatively large sample. STM also has drawbacks; it is a surface sensitive method and the interaction between the scanning tip and the surface may induce changes in the surface. However, the method is certainly capable of revealing details like nano-domains, which might due to their small sizes and averaging within experimental coherence regions be overlooked by other methods. This by no means reduces the importance of the alternative methods, but rather requires a comparison of all results, which should lead to a single acceptable conclusion.

Although the major contribution to the surface density of states in $NbSe_3$ is supposed to come from the corrugated top Se layer [41], it should be taken into account that a charge distribution can also be detected over larger distances and may show details located below the surface. Such effects have been observed before in the case of layered transition-metal dichalcogenides [46,47]. As schematically shown in Fig. 2(a) and in the insets, the observed long-range ordering in $NbSe_3$ [41] can be explained by beating of two overlapped CDWs. A periodicity of $116\boldsymbol{b_0}$ is shown along both columns ($58\boldsymbol{b_0}$ accommodates $14\boldsymbol{q_1}$ and $15\boldsymbol{q_2}$ CDW modulation periods [43]). The first half of the top column is modulated with $\boldsymbol{q_2}$ and the second half with $\boldsymbol{q_1}$, while the column below is modulated in the opposite way. If both overlapped modulations are indeed detected, STM will show the characteristic beating. If in addition the $\boldsymbol{q_2}$ sections are statistically displaced by half shorter $\boldsymbol{q_1}$ sections ($7\boldsymbol{q_1}$ periods extend over $29\boldsymbol{b_0}$ only [30]), as shown in Fig. 2(b), the close proximity of the two columns would result in a $\boldsymbol{q_1}$ contribution to the diffraction pattern only [43]. However, the $\boldsymbol{q_2}$ sections would still be detected by STM.

All details revealed by LT STM, together with the results of the alternative methods, seem to support a partly modified domain model. According to this, the $\boldsymbol{q_1}$ and $\boldsymbol{q_2}$ CDW segments are still statistically interchanged along the type-III columns bellow T_1 and in addition along the type-I columns below T_2. Such a disorder triggers the formation of unstable CDW domains with the characteristic twinkling in the satellite dark field TEM images. Since the type-III pairs of columns form slabs parallel to the $\boldsymbol{a_0}$–$\boldsymbol{b_0}$ plane, a long range CDW ordering takes place on cooling along these slabs first (between T_1 and T_2). However, contrary to the original predictions [43] the LT STM results may suggest that the strongly bonded pairs of columns are alternatively modulated by the $\boldsymbol{q_1}$ and $\boldsymbol{q_2}$ CDWs. If so, such pairs of columns in fact represent the basic structural elements, which are ordered or disordered on a nanoscale. Consequently, layered domains of modulated BCTP columns are indeed formed parallel to the $\boldsymbol{b_0}$–$\boldsymbol{c_0}$ plane, but are composed of adjacent $\boldsymbol{q_1}$ and $\boldsymbol{q_2}$ sublayers, which can easily be interchanged as part of the unstable domain structure.

6. Conclusions

The details discussed raise questions regarding a number of aspects of the CDW states in $NbSe_3$. The origin of the peculiar CDW ordering in $NbSe_3$ seems to be in its basic structure, composed of symmetry related pairs of BCTP columns.

The suggested explanation seems to be in accord with the available experimental evidence, particularly with the LT STM results [39,41], including the recently reported surface dependence of the T_2 transition temperature [42].

Further experimental and theoretical studies are needed to advance our understanding of the physical reasons for the unique behaviour of CDWs in $NbSe_3$.

Acknowledgements

Financial support of the Slovenian Research Agency (ARRS) (AP, HJPvM, RŽ and EZ) and of the Natural Sciences and Engineering Research Council of Canada (JCB) is gratefully acknowledged.

References

[1] A.H. Thompson, A. Zettl, G. Grüner, Phys. Rev. Lett. 47 (1981) 64–67.
[2] A. Zettl, C.M. Jackson, A. Janossy, G. Grüner, A. Jacobsen, A.H. Thompson, Solid State Commun. 43 (1982) 345–347.
[3] Z.Z. Wang, M.C. Saint-Lager, P. Monceau, M. Renard, P. Gressier, A. Meerschaut, L. Guemas, J. Rouxel, Solid State Commun. 46 (1983) 325–328.
[4] Z.Z. Wang, P. Monceau, M. Renard, P. Gressier, L. Guemas, A. Meerschaut, Solid State Commun. 47 (1983) 439–443.
[5] J. Dumas, C. Schlenker, J. Marcus, R. Buder, Phys. Rev. Lett. 50 (1983) 757–760.
[6] J.P. Pouget, S. Kagoshima, C. Schlenker, J. Marcus, J. Phys. (Paris) Lett. 44 (1983) 113–120.
[7] M. Ganne, A. Boumaza, M. Dion, J. Dumas, Mater Res. Bull. 20 (1985) 1297–1308.
[8] B.T. Collins, K.V. Ramanujachary, M. Greenblat, Solid State Commun. 56 (1985) 1023–1028.
[9] R.C. Lacoe, H.J. Schulz, D. Jérome, K. Bechgaard, I. Johannsen, Phys. Rev. Lett. 55 (1985) 2351–2354.
[10] S.J.L. Billinge, http://physics.aps.org/articles/v3/25 (2010) 1–6;
M.J. Cliffe, M.T. Dove, D.A. Drabold, A.L. Goodwin, Phys. Rev. Lett. 104 (2010) 125501-1–125501-4.
[11] J.L. Hodeau, M. Marezio, C. Roncan, R. Ayroles, A. Meerschaut, J. Rouxel, P. Monceau, J. Phys. C: Solid State Phys. 11 (1978) 4117–4134.
[12] J.A. Wilson, Phys. Rev. B 19 (1979) 6456–6468.
[13] N.P. Ong, P. Monceau, Phys. Rev. B 16 (1977) 3443–3455.
[14] G. Grüner, Density Waves in Solids, Addison-Wesley, Reading, MA, 1994.
[15] P. Monceau, N.P. Ong, A.M. Portis, A. Merschaut, J. Rouxel, Phys. Rev. Lett. 37 (1976) 602–605.
[16] R.M. Fleming, C.C Grimes, Phys. Rev. Lett. 42 (1979) 1423–1426.
[17] P. Monceau, in: P. Monceau (Ed.), Electronic Properties of Inorganic Quasi-One-Dimensional Matals, Part II, D. Reidel, Dordrecht, 1985, p. 139.
[18] R.L. Withers, J.A. Wilson, J. Phys. C 19 (1986) 4809–4845.
[19] A. Ayari, R. Danneau, H. Requardt, L. Ortega, J.E. Lorenzo, P. Monceau, R. Currat, S. Brazovskii, G. Grübel, Phys. Rev. Lett. 93 (2004) 106404-1–106404-4.
[20] Y.S. Hor, Z.L. Xiao, U. Welp, Y. Ito, J.F. Mitchell, R.E. Cook, W.K. Kwok, G.W. Crabtree, Nano Lett. 5 (2005) 397–401.
[21] C. Schlenker, J. Dumas, M. Greenblatt, S. van Smaalen (Eds.), Physics and Chemistry of Low-Dimensional Inorganic Conductors, in: 354 NATO Advanced Studies Institute Series B: Physics, Plenum, NY, 1996.
[22] Proceedings of the International Workshop on Electronic Crystals, ECRYS 2008, Cargèse, France, 2008. Physica B 404 (2009).
[23] R.E. Thorne, Phys. Rev. B 45 (1992) 5804–5810.
[24] R. Danneau, A. Ayari, D. Rideau, H. Requardt, J.E. Lorenzo, L. Ortega, P. Monceau, R. Currat, G. Grübel, Phys. Rev. Lett. 89 (2002) 106404-1–106404-4;
R.E. Thorne, J.D. Brock, M. Sutton, Phys. Rev. Lett. 91 (2003) 049703-1;
R. Danneau, A. Ayari, D. Rideau, H. Requardt, J.E. Lorenzo, L. Ortega, P. Monceau, R. Currat, G. Grübel, Phys. Rev. Lett. 91 (2003) 049704-1.
[25] E. Slot, H.S.J. van der Zant, K. O'Neill, R.E. Thorne, Phys. Rev. B 69 (2004) 073105-1–073105-4.
[26] K. O'Neill, E. Slot, R.E. Thorne, H.S.J. van der Zant, Phys. Rev. Lett. 96 (2006) 096402-1–096402-4.

[27] A.F. Isakovic, P.G. Evans, J. Kmetko, K. Cicak, Z. Cai, B. Lai, R.E. Thorne, Phys. Rev. Lett. 96 (2006) 046401-1–046401-4.
[28] K. Tsutsumi, T. Takagaki, M. Yamamoto, Y. Shiozaki, M. Ido, T. Sambongi, K. Yamaya, Y. Abe, Phys. Rev. Lett. 39 (1977) 1675–1676.
[29] R.M. Fleming, D.E. Moncton, D.B. McWhan, Phys. Rev. B 18 (1978) 5560–5563.
[30] A.H. Moudden, J.D. Axe, P. Monceau, F. Lévy, Phys. Rev. Lett. 65 (1990) 223–226.
[31] S. Rouzière, S. Ravy, J.P. Pouget, R.E. Thorne, Solid State Commun. 97 (1996) 1073–1077.
[32] S. van Smaalen, J.L. de Boer, A. Meetsma, H. Graafsma, H.-S. Sheu, A. Darovskikh, P. Coppens, F. Lévy, Phys. Rev. B 45 (1992) 3103–3106.
[33] F. Devreux, J. Phys. (Paris) 43 (1982) 1489–1495.
[34] J.H. Ross Jr., Z. Wang, C.P. Slichter, Phys. Rev. Lett. 56 (1986) 663–666.
[35] S. Suh, W.G. Clark, P. Monceau, R.E. Thorne, S.E. Brown, Phys. Rev. Lett. 101 (2008) 136407-1–136407-4.
[36] J. Schäfer, Eli Rotenberg, S.D. Kevan, P. Blaha, R. Claessen, R.E. Thorne, Phys. Rev. Lett. 87 (2001) 196403-1–196403-4.
[37] J. Schäfer, M. Sing, R. Claessen, Eli Rotenberg, X.J. Zhou, R.E. Thorne, S.D. Kevan, Phys. Rev. Lett. 91 (2003) 066401-1-066401-4.
[38] K.K. Fung, J.W. Steeds, Phys. Rev. Lett. 45 (1980) 1696–1699.
[39] Z. Dai, C.G. Slough, R.V. Coleman, Phys. Rev. Lett. 66 (1991) 1318–1321;
S. van Smaalen, J.L. de Boer, P. Coppens, H. Graafsma, Phys. Rev. Lett. 67 (1991) 1471;
Z. Dai, C.G. Slough, R.V. Coleman, Phys. Rev. Lett. 67 (1991) 1472.
[40] C. Brun, Z.Z. Wang, P. Monceau, J. Phys. IV (France) 131 (2005) 225–226.
[41] C. Brun, Z.Z. Wang, P. Monceau, Phys. Rev. B 80 (2009) 045423-1–045423-11.
[42] C. Brun, Z.Z. Wang, P. Monceau, S. Brazovskii, Phys. Rev. Lett. 104 (2010) 256403-1- 256403-4.
[43] A. Prodan, N. Jug, H.J.P. van Midden, H. Böhm, F.W. Boswell, J.C. Bennett, Phys. Rev. B 64 (2001) 115423-1–115423-6.
[44] R.M. Fleming, C.H. Chen, D.E. Moncton, J. de Phys. (Paris) 44 (1983) C3-1651–C3-1658.
[45] H. Lüth, Surfaces and Interfaces of Solid Materials, Springer, Berlin, 1995, p. 207.
[46] A. Prodan, V. Marinković, M. Rojšek, N. Jug, H.J.P. van Midden, F.W. Boswell, J.C. Bennett, H. Böhm, Surf. Sci. 476 (1–2) (2001) 71–77.
[47] D. Cukjati, A. Prodan, N. Jug, H.J.P. van Midden, S.W. Hla, H. Böhm, F.W. Boswell, J.C. Bennett, Phys. Status Solidi (a) 193 (2002) 246–250.